

# Pavement condition prediction modeling using artificial neural networks

---

---

### 8.1. Introduction

Estimation of pavement's structural health condition is one of the most important aspects to optimize Pavement Management Systems (PMS). Assuming that poor structural health would be eventually reflected by the deterioration in functional performance indicators, the consideration of structural aspect is often ignored. In real field conditions, visual distresses usually get reflected after a major portion of the pavement structure is deteriorated. In such cases, any sort of maintenance or rehabilitation activity would be expensive and would require a substantial amount of time, resources, and efforts. On the other hand, the prior inclusion of structural condition during any decision-making process would provide warning signs during the early stages of pavement deterioration and addressing them may demand only minor repairs which would save huge funds.

Applications of non-destructive testing devices such as Falling Weight Deflectometer (FWD) provide crucial estimates of structural health of pavements. FWD assesses not only the structural adequacy but also provide substantial information about pavement layers and its subsurface conditions, including subgrade. Thus, most of the highway agencies prefer FWD testing as a part of their routine pavement assessment procedures that are usually scheduled at periodic intervals. However, the estimation of layer moduli demands back-calculation of FWD data, and its accurate analysis requires technical expertise with exact estimates of pavement layer thicknesses, which is either done through coring or Ground-Penetrating Radar (GPR) scans. The use of GPR is not a common practice in India, and coring practices require considerable time and resources. Furthermore, the practice of data acquisition at frequent intervals is indeed time-consuming, labor-intensive, interrupts traffic, and expensive, hence, it is difficult to be performed repeatedly. These are possibly a few of the contributing reasons in neglecting the structural aspect of pavements during the selection of maintenance or repair decisions. Therefore, to cope up with these

limitations, application of Deflection Basin Parameters (DBP) that are indicative of pavement deflection basin, and eventually its strength is highly useful.

Although a lot of research has been done, the studies on the inclusion of diversified factors with techniques of computational intelligence to address the real-life challenges of field testing in pavement prioritization are limited. Therefore, an attempt to explore the amalgamation of DBP with neural networks to ease the task of data analysis is developed in this chapter. It offers an attractive way to inspire the practice of incorporating strength parameters in pavement prioritization projects. A thorough review of literature helped to ascertain typical deflection basin parameters and range of their values, as proposed by the researchers (Chang et al., 2014). To inculcate the effect of upper as well as lower pavement layers, two DBP, namely Surface Curvature Index (SCI), and Base Curvature Index (BCI) are used in conjunction with eight decision variables in this work.

SCI is defined as the difference between the deflections measured by the sensor located at the center of the load plate and another sensor located at 300 mm from the center. This is a measure of the structural quality of the upper pavement layers, specifically asphalt layers (Kim, 2000). Similarly, BCI infers the quality of lower layers and subgrade. It is defined as the difference between the deflections measured by the sensor located 600 mm and 900 mm from the center of the load plate. Thus,

$$SCI = D_0 - D_{300}$$

$$BCI = D_{600} - D_{900}$$

where, D represents the deflection measured at sensor locations (in mm) indicated at the subscript of D. Table 8.1 enlists threshold range of DBP used in this study, as found in the literature.

**Table 8.1. Threshold ranges of layer condition for SCI and BCI**

Parameter	Concerned layer	Layer condition threshold range (mils)				
		Very good	Good	Fair	Poor	Very poor
SCI	Asphalt layer	<4	4-6	6-8	8-10	>10
BCI	Base layer	<2	2-3	3-4	4-5	>5

*Source:* Compiled from Chang et al. (2014).

This chapter presents an alternative means for more efficient usage of DBP, and the potential of Artificial Neural Networks (ANN) modeling to predict DBP and ascertain the structural condition of pavements is investigated. Four basic requirements for developing reliable prediction models are adequate database, factors affecting performance, form of model, and a method to assess the precision and accuracy of the model. In accordance with this, the database consisting of different performance parameters has been sufficiently obtained through FWD testing. The models are developed using artificial neural networks and assessed on the basis of coefficient of determination along with mean square error estimates. The superiority of ANN models is highlighted by comparing their results with the multiple linear regression approach.

## **8.2. Data collection using FWD testing**

In order to create robust models using neural networks, a comprehensive and accurate database is a prerequisite. Therefore, for this study, a vast road network of 124 km was selected for testing and modeling purpose in India. The selection was primarily done on the basis of pavement condition, and observation of visual distresses such as fatigue cracking, raveling, rutting, and lane/shoulder drop off. After the selection of pavement sections, detailed field surveys and testing were performed to collect the required data.

Field tests to measure structural adequacy were conducted in accordance with the standards of Indian road congress using Dynatest model 8000 FWD and load plate of diameter 300 mm (IRC 115, 2014). The geophone configuration is decided as per the need at the location and standards, which is taken to be 0, 200, 300, 600, 900, and 1200 mm in this study (IRC 115, 2014). Three drops of mass were taken at each testing point with loading time for each drop generally in the range of 0.015-0.050 s, and the first drop being the seating load, was not recorded. The deflection data has been normalized as per the standard load, and suitable corrections for temperature have been applied. FWD testing was carried out at every 100 m intervals approximately. At a few locations where pavement condition was poor, the testing interval was reduced to incorporate greater number of testing points to gain a better understanding of the pavement structure. This resulted in a total of 1452 test records. In-situ asphalt surface temperature and air temperature were recorded at the time of FWD testing.

Further details of the FWD and testing procedure can be found elsewhere in the literature (ASTM D4694-09, 2015; ASTM D4695-03, 2015; IRC 115, 2014). Figure 8.1 shows a typical FWD deflection basin obtained from data recorded at a test location. The position of load drop, radial geophone offsets, and deflections ( $D_0$  to  $D_5$ ) measured at the corresponding positions of sensor locations are also shown along with the expressions for estimation of SCI and BCI.

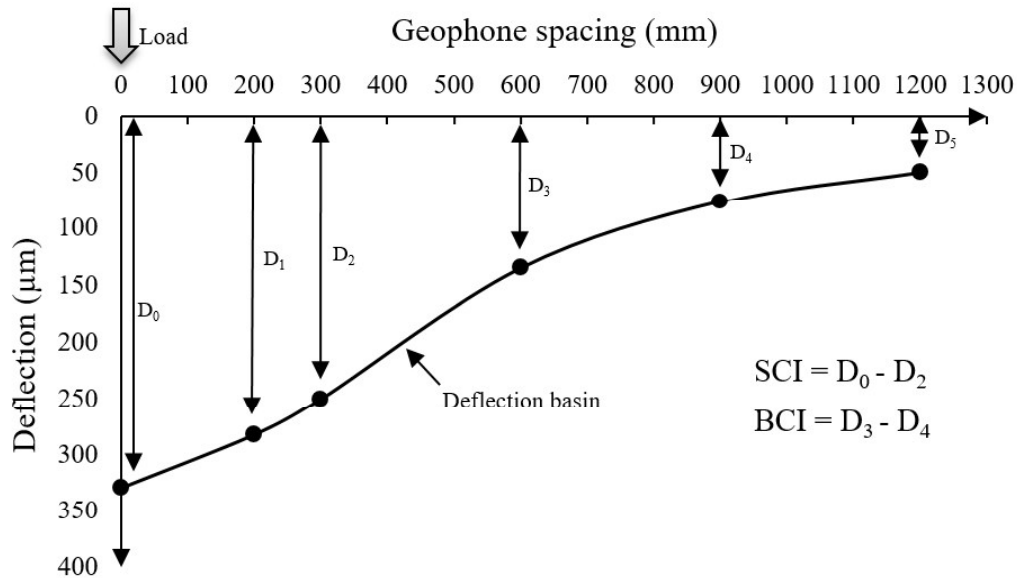


**Figure 8.1. A typical FWD deflection basin and geophone spacing used in this study**

International Roughness Index (IRI) is a standardized roughness measurement of the longitudinal profile of a traveled wheel path, and it is commonly measured in the unit m/km (Papagiannakis & Masad, 2008). The data was collected using a bump integrator. A high value of IRI indicates increased roughness level and vice-versa. Subgrade soil parameters, including California Bearing Ratio (CBR) and Maximum Dry Density (MDD), were determined through the laboratory tests on soil samples collected from test pits. CBR test is a penetration test which intends to determine the strength of subgrade soil, as compared to standard crushed rock (AASHTO T 193, 1993). High CBR value indicates a high strength of the soil. Soaked CBR values at 56 blows are taken in this study. MDD is the value of dry density corresponding to optimum moisture content. Table 8.2 summarizes a sample of laboratory testing results conducted on the subgrade soil. Coring operations along with test pits and field surveys were performed to collect the facts about the type and thickness of layers, crack propagation and de-lamination (if any), characterization of materials,

and subsurface drainage conditions. Measurement of deflections, IRI, and distresses was performed at the same location to maintain uniformity and reliability in the results. The points at which data was missing, linear interpolation was adopted.

**Table 8.2. A sample of laboratory testing results on subgrade soil**

Test pit number	Grain size analysis			Atterberg limits		Soil class	Field moisture content (%)	Field dry density (g/cm <sup>3</sup> )	Heavy compaction test		CBR (%)
	4.75 mm IS Sieve	425 mic IS Sieve	75 mic IS Sieve	LL	PI				MDD (g/cm <sup>3</sup> )	OMC (%)	
1	92	84	78	26	20	CL	8.98	1.70	1.95	11.00	29.2
2	100	93	88	30	14	CL	8.53	1.70	1.98	9.70	14.6
3	93	89	84	25	6	ML-CL	19.11	1.83	1.97	10.00	46.7
4	93	88	69	33	9	ML	1.54	1.85	1.88	10.50	21.5
5	100	94	71	24	6	ML-CL	10.57	1.84	1.99	10.50	46.7

### 8.2.1. Selection of decision variables

In this work SCI and BCI are taken as output, and input variables include pavement structure-related factors such as thickness of asphalt layer ( $L_a$ ), thickness of base layer ( $L_b$ ), and total thickness of pavement ( $L_t$ ); functional performance factor such as IRI; subgrade soil strength depicting factors such as MDD and CBR; lastly environmental factors including atmospheric temperature ( $T_a$ ), and asphalt pavement surface temperature at the time of testing ( $T_s$ ). Review of literature helped to ascertain the domains which directly or indirectly affect the structural condition of pavements (Sollazzo et al., 2017). Accordingly, the input variables are selected from the wide spectrum of important attributes. The selection also depends upon the availability and ease of collecting data for these attributes. Pertaining to the ease of conducting FWD or CBR test, it should be noted that FWD is limited in its availability while CBR is widely available. Due to the limited availability of FWD for conducting field inspections anywhere in the country, it needs to be transported from place to place. Performing this task repeatedly is neither easy nor economical, and needs proper planning along with sufficient funds. On contrary, conducting CBR tests is relatively easy and economical since it can be performed at multiple places due to its wide availability. The advantage of developing a prediction model is that in case of difficulty in procuring any particular device or conducting test, the particular parameter can be dropped off

from the model whereas field tests including FWD, do not avail such flexibility and entire testing procedure from data collection to its analysis, needs to be followed every time. The present study aims to provide an approach to alleviate the need of conducting FWD tests repeatedly. It offers an idea to incorporate the parameters from diverse field to develop the robust prediction models which are highly flexible in nature since its parameters can be suitably varied or modified according to the intended problem. The complete methodology is demonstrated by using the selected set of parameters. However, the input variables can be always varied according to the scope of work, equipment availability, ease, and time constraints.

To simplify the research, the dataset does not include the particulars of maintenance or rehabilitation activities. In addition to this, due to the limited accessibility to the previous records, time constraint, and scope of work; pavement construction history data, and estimation of traffic loading could not be included in the work, which can be taken in future studies. Nevertheless, with the available resources itself, significant information was collected, and a substantial amount of dataset for modeling purposes could be generated.

### **8.3. Development of ANN prediction model**

ANN models work on the principle of the biological neural network of the human brain and analogous to its thought process, which has the capability to learn and compensate for errors (Karayiannis & Venetsanopoulos, 1993). The central processing units of ANN networks are called neurons which have weighted connections between them to receive input data, process and transfer the data as output to other neurons. They can learn input-output mapping and provide an easy approach to estimate solutions of complex and non-linear problems without any need for preliminary conjectures. Improved performance of these models could be attained by defining more levels of input processing based on trial-and-error methods, and repeatedly training the networks. Further, accurate results can be obtained by comparing outputs from different training algorithms. However, generating a realistic ANN network requires empirical experiences; its effectiveness is entirely based on the trial-and-error process, and repeatability of results is not assured (Zain et al., 2010). Despite the fact that the development of these models is trial-and-error based, it is still essential to carefully select the critical governing parameters according to the nature

of the problem. ANN follows the black-box approach and therefore, the nature of the prediction equation is not known (Sollazzo et al., 2017).

### **8.3.1. Selection of ANN model parameters**

#### **8.3.1.1. Network**

A set of layers and nodes form the major components of an ANN network structure. Commonly, a multilayer feed-forward neural network is used. The network consists of an input layer, one or more hidden layers which act as a boundary layer between the input and output layers and contains computational nodes called neurons, activation functions, bias, and output layer. The type of network structure adopted in this study is exemplified in Figure 8.2. It has 8 neurons in the input layer corresponding to 8 decision variables (X):  $L_a$ ,  $L_b$ ,  $L_t$ ,  $T_s$ ,  $T_a$ , CBR, MDD, and IRI; used in this study,  $m$ ,  $n$ , and  $p$  represents neurons in the first, second, and  $i^{th}$  hidden layer, respectively, and finally one neuron in the output layer corresponding to SCI or BCI, as per the case under consideration. Assuming the multilayer feed-forward network, its structure could be defined as 8-m-n-p-1 structure. Figure 8.2 also depicts the processing inside a neuron, wherein the net input along with their respective weights (W) is summed with respective biases, and the selected transfer function is applied over it (logsig transfer function in the present study). The arrows show the forward flow of information and back-propagation of errors during the training phase. The back-propagation mechanism propagates the errors in the reverse direction, updates biases and weights, and minimizes error after every iteration (Karayiannis & Venetsanopoulos, 1993).

Literature shows that researchers have applied various structures for the ANN model to obtain the best prediction performance (Amin & Amador-Jimenez, 2016; Shafabakhsh et al., 2015). The process of selection of the best network structure is usually done by varying the two important parameters, namely the number of hidden layers and number of neurons in the hidden layer(s), but it is subjected to the complexity of various other parameters including computation memory and time. Authors of similar previous studies varied the number of nodes of the hidden layer, such as 5, 10, and 25, based on trial-and-error (Fakhri & Dezfoulian, 2019; Sollazzo et al., 2017). As far as this study is concerned, different network structures are developed by varying the two parameters mentioned above and their results are compared to obtain the optimum structure. The

best network structure is then recommended for such similar studies concerned with the computation of structural parameters of asphalt pavements. Following the recommendation regarding the number of nodes in hidden layer to be  $i/2$ ,  $1(i)$ ,  $2(i)$ , and  $(2i + 1)$ , where  $i$  is the number of input nodes, different structures are tried with number of nodes as  $8/2=4$ ,  $1(8)=8$ ,  $2(8)=16$  and  $(2*8+1)=17$  (Zhang et al., 1998). For the sake of avoiding complexity in the architectures, the hidden layers are kept up to a maximum number of two. As depicted in Figures 8.3 and 8.4, the different ANN architectures tried with one and two hidden layers are 8-4-1, 8-8-1, 8-16-1, 8-17-1, 8-4-4-1, 8-8-8-1, 8-16-16-1 and 8-17-17-1.

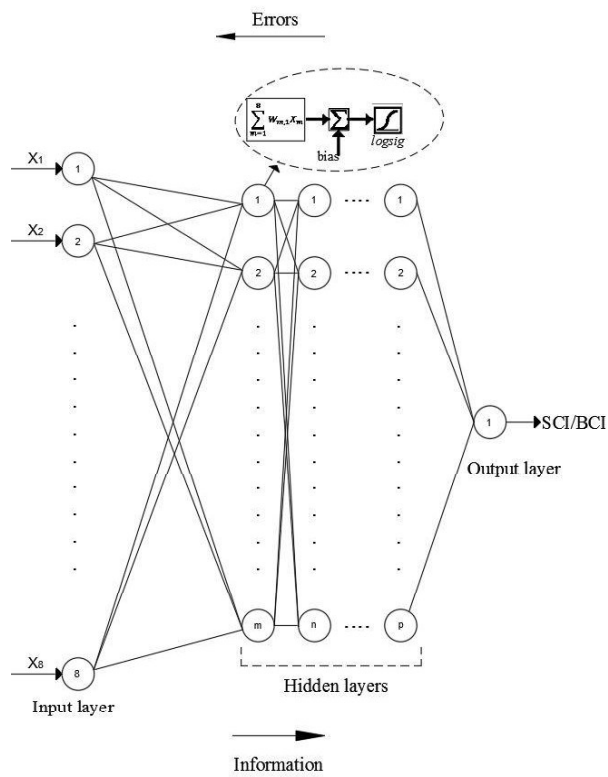
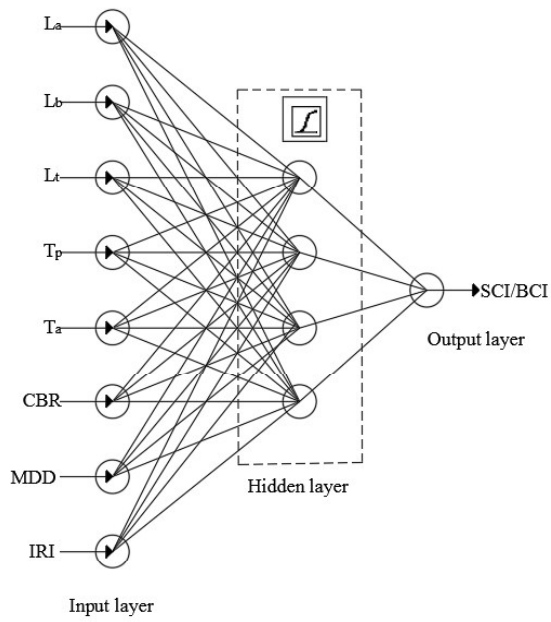
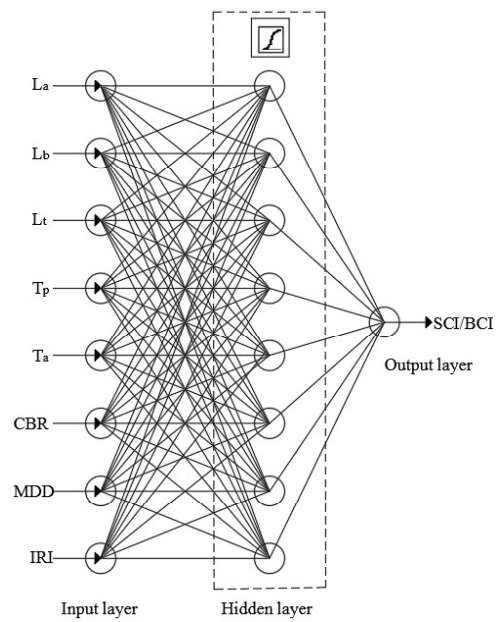


**Figure 8.2. Illustration of ANN structure and its neuron**

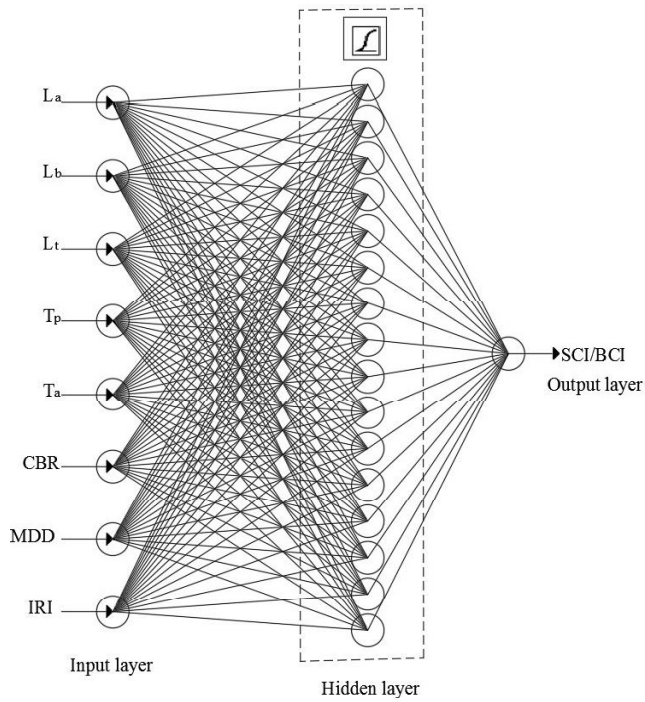




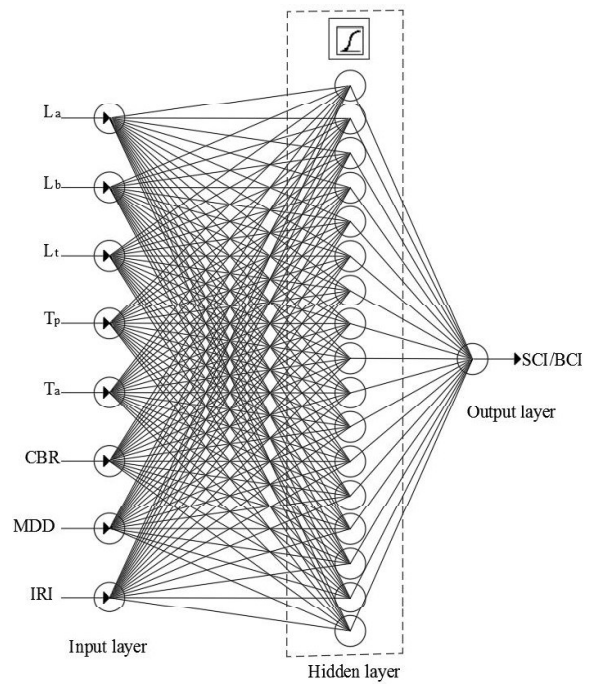
(a) 8-4-1



(b) 8-8-1

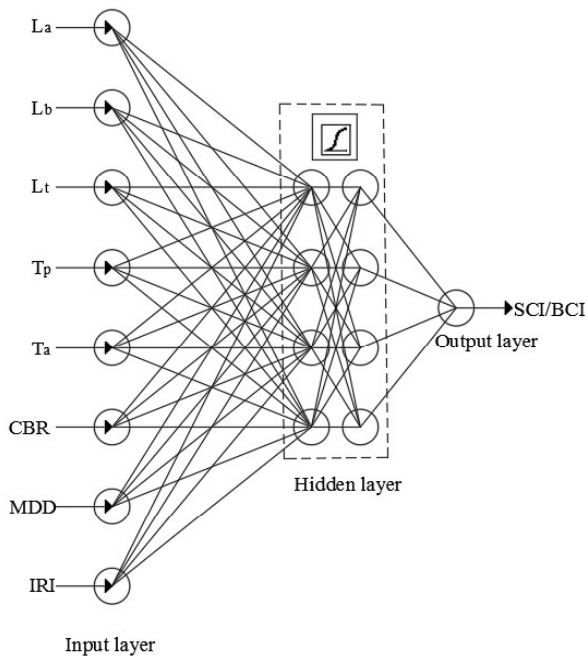


(c) 8-16-1

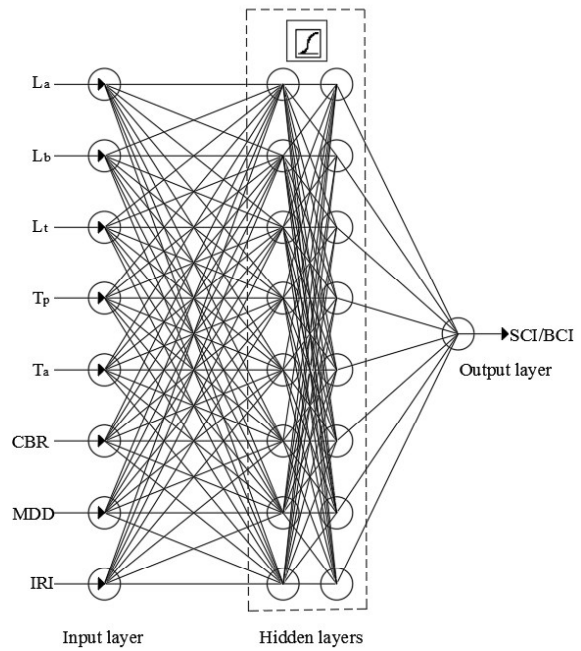


(d) 8-17-1

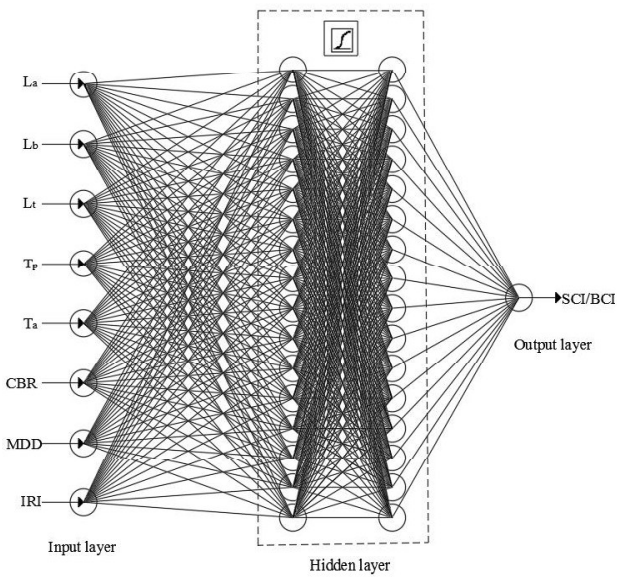
Figure 8.3. ANN architectures with one hidden layer



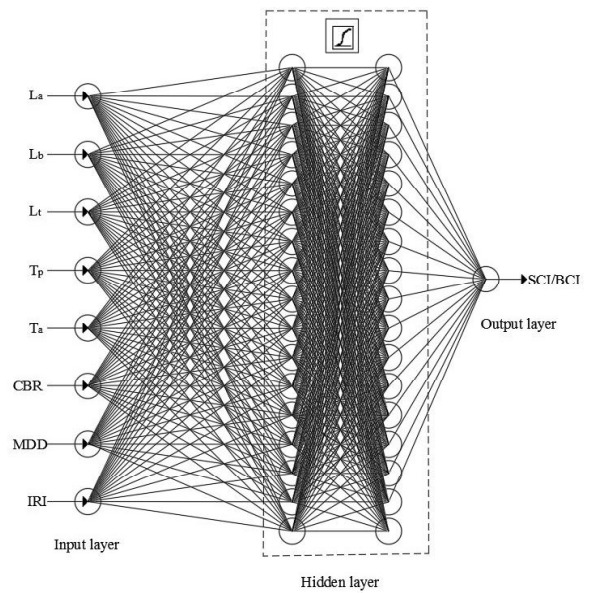
**(a) 8-4-4-1**



**(b) 8-8-8-1**



**(c) 8-16-16-1**



**(d) 8-17-17-1**

**Figure 8.4. ANN architectures with two hidden layers**

### 8.3.1.2. *Training, validation and testing dataset*

Since ANN learns and adapts from the input data, a more accurate model will result from more number of training data points. This seems to be a feasible solution for a synthetic database where the dataset is generated from any simulation framework. However, the data used in the present study is taken from the actual pavement testing, which is subjected to cost and time constraints. Recent studies have helped to ascertain the division of input data (Fakhri & Dezfoulian, 2019; MATLAB & Simulink, 2020; Sollazzo et al., 2017). Accordingly, the input data is divided into three sets by considering a typical ratio of training (70%), validation (15%), and testing (15%) for 124 km of pavement with total 1452 data points. Furthermore, it is advisable to perform normalization of the data before the training and testing process to bring the variables in the standard range of 0 to 1 or -1 to 1 in order to avoid computational problems. Therefore, in the initial step, all the raw data has been normalized, using Eq. (8.1) (Sanjay & Jyothi, 2006):

$$x_i = \frac{0.8}{(x_{max} - x_{min})} * (x_i - x_{min}) + 0.1 \quad (8.1)$$

where  $x_{max}$  and  $x_{min}$  are the maximum and minimum values of the data, respectively and  $x_i$  is the  $i^{th}$  data point of the dataset.

### 8.3.1.3. *Network algorithm and its associated functions*

Many different network algorithms for ANN models are available, such as Radial Basis, Perceptron, Cascade-forward BP, Feed-forward time-delay, Feed-forward distributed time-delay, and self-organizing map (Demuth & Beale, 2004). Feed-forward Back-Propagation (BP) algorithm is widely used for its application in problems of pavement engineering (Elbagalati et al., 2018; Li & Wang, 2018; Sollazzo et al., 2017). For the feed-forward BP algorithm, the widely-adopted transfer functions are log-sigmoid transfer function (logsig), hyperbolic tangent sigmoid transfer function (tansig), and linear transfer function (purelin). Non-linear relationships between input and output variables would be better addressed by using non-linear transfer function such as sigmoid function. Therefore, the logsig transfer function is adopted in this study, as given by Eq. (8.2):

$$z = \frac{1}{1 + e^{-y}} \quad (8.2)$$

where  $z$  is the output from the hidden layer neuron after sigmoid function, and  $y$  is the net input to the hidden layer neuron.

Eventually, the BP algorithm reduces the error and finds its lowest possible value, which is represented by performance function. This includes Mean Square Error (MSE), Sum Square Error (SSE), Mean Absolute Error (MAE), Root Mean Squared Error (RMSE), and Mean Absolute Percentage Error (MAPE). Previous studies have mostly applied MSE performance function, and the same has been considered in this study. MSE of  $n$  data points is given by Eq. (8.3):

$$MSE = \frac{1}{n} \sum_{i=1}^n (O_i - P_i)^2 \quad (8.3)$$

where  $O_i$  and  $P_i$  are the observed and predicted values of any data point, respectively.

In order to reduce the error, as the number of iterations proceeds, the weights and biases are continuously updated in which optimum values of learning rate, and momentum provides better accuracy as well as faster convergence. The default values of these parameters is adopted. Training function and learning function also govern the reduction in error. Training functions are based on gradient descent algorithm (traingd, traingda, traingdx), Bayesian regularization (trainbr) or Levenberg–Marquardt BP (trainlm), and learning functions such as learngd (gradient descent weight/bias learning function), learngdm (gradient descent with momentum weight/bias learning function), etc. are used. In this work, trainlm and learngd are used as training and learning functions, respectively.

Figure 8.5 presents the step-wise methodology for developing ANN models in this study based on the discussion presented in preceding paragraphs.

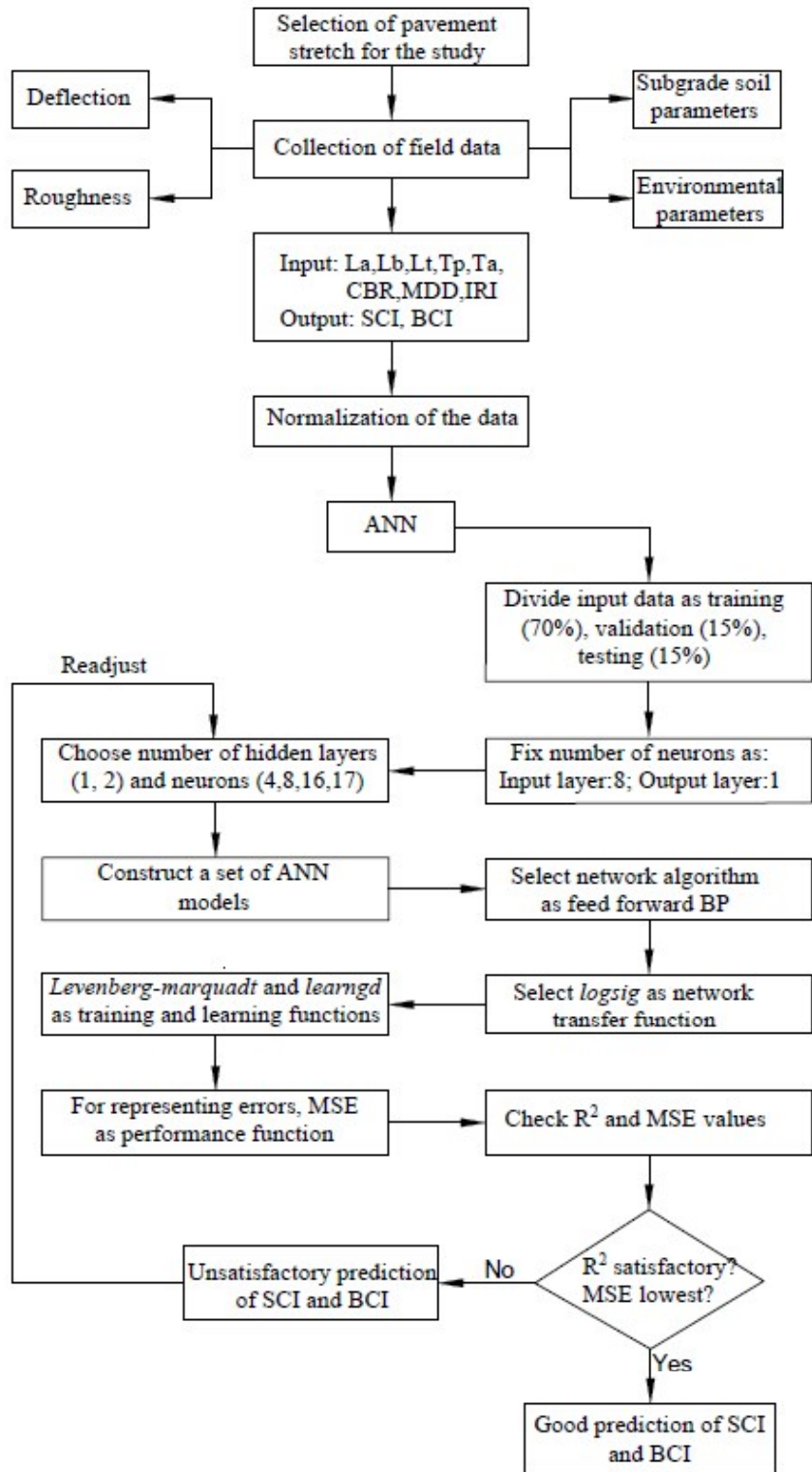
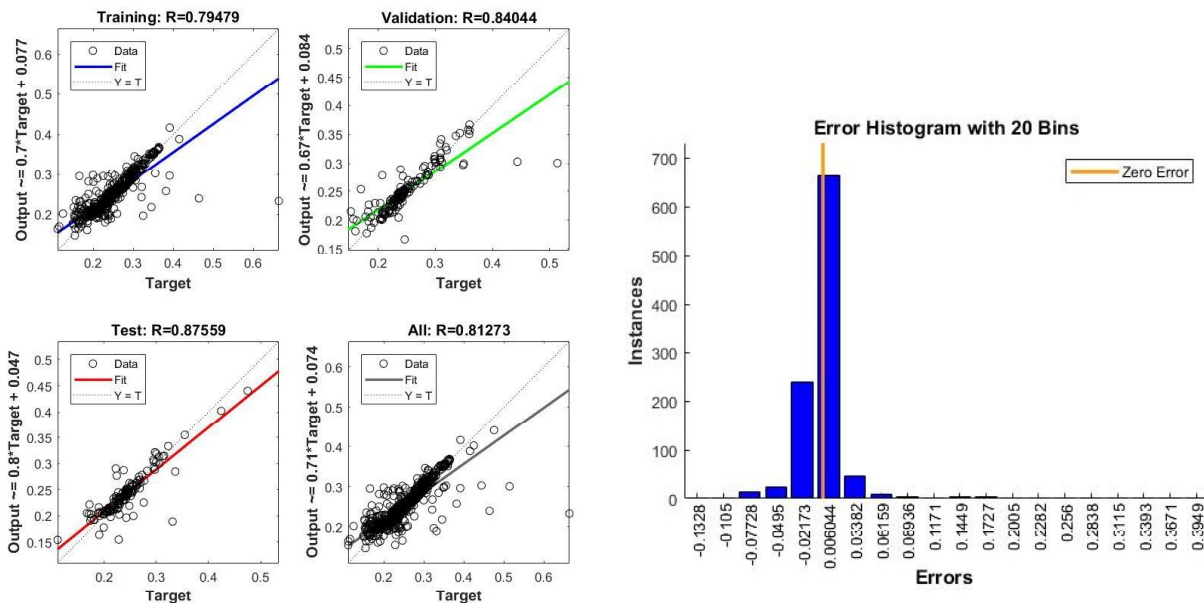


Figure 8.5. Flow chart showing ANN model development in the study

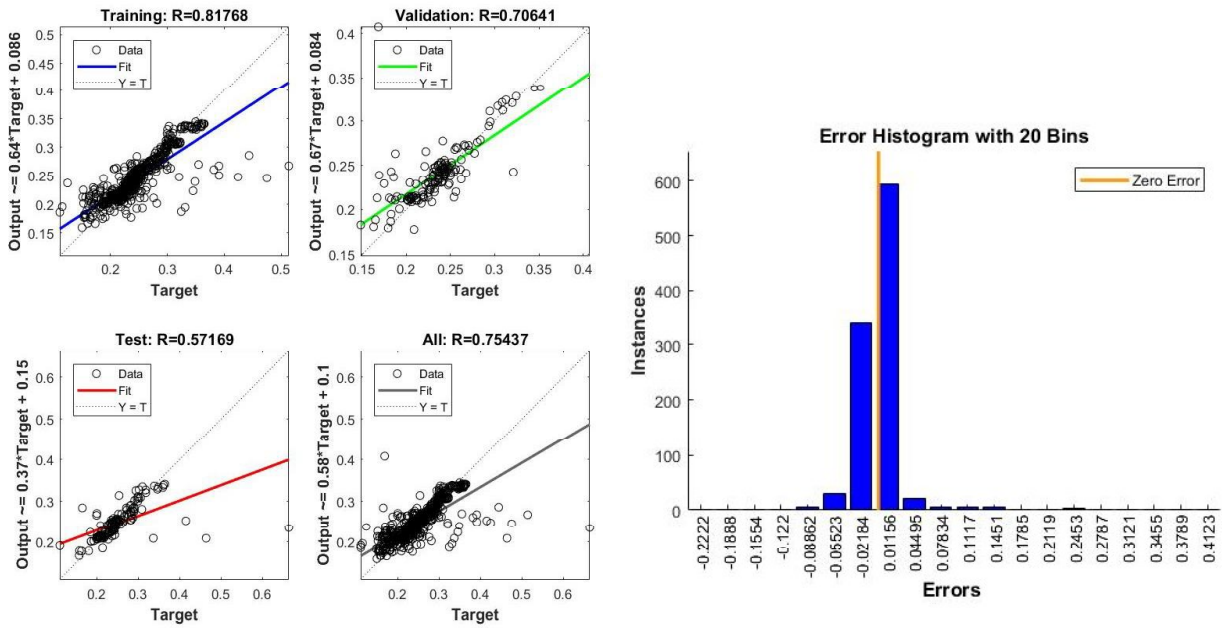
### 8.3.2. ANN Results

In order to illustrate the efficacy of ANN models in predicting the structural parameters of asphalt pavements, eight different models each for the two output variables are trained, resulting in a total of sixteen models. The proposed structures differ in the number of hidden layers and neurons in these layers, with the input and output layer fixed with eight and one nodes, respectively corresponding to eight input and one output variable. The entire analysis is performed in MATLAB software, version R2017a (Demuth & Beale, 2004).

The regression charts for training, validation, and testing phases along with error histograms for two model architectures 8-8-1 and 8-8-8-1, as an example, are presented in Figures 8.6 and 8.7 for SCI and BCI, respectively. The remaining charts are presented in Appendix-3. The error histograms plotted for each ANN architecture reveal that their average is very close to zero, and in almost all the cases, 80% of the errors or more are confined within one or two central bins. The performance of these models is summarized in Table 8.3.

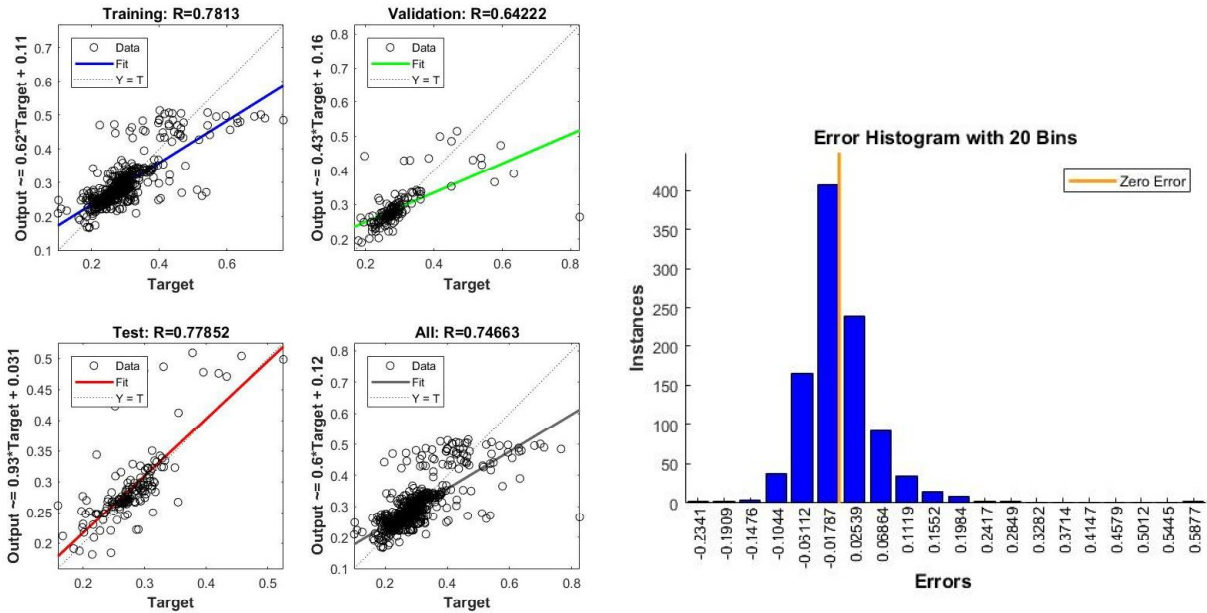


(a) 8-8-1

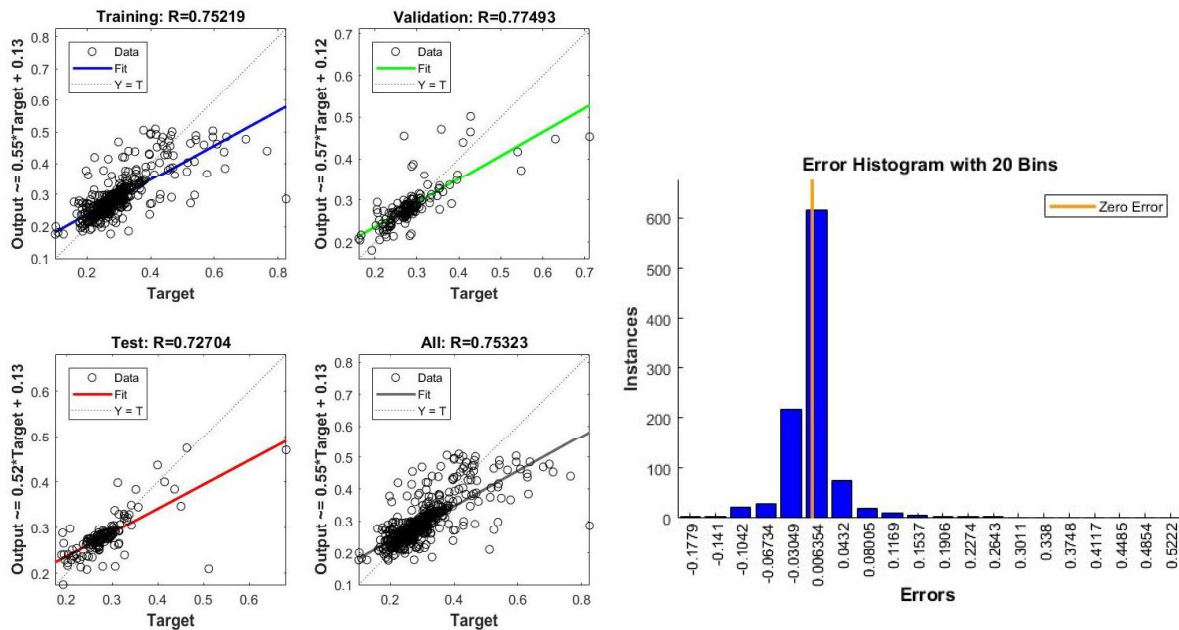


(b) 8-8-1

Figure 8.6. Regression results and error histograms for SCI using 8-8-1 and 8-8-8-1 network structures



(a) 8-8-1



(b) 8-8-8-1

Figure 8.7. Regression results and error histograms for BCI using 8-8-1 and 8-8-8-1 network structures

Table 8.3. Performance results of different ANN models

Network	Input variables	Neurons	Output variables	MSE	Stage	R <sup>2</sup>
8-4-1	La, Lb, Lt, Tp, Ta, CBR, MDD, IRI	4	SCI	0.0860	Training	0.719
					Validation	0.771
					Test	0.786
					Total	0.734
8-8-1	La, Lb, Lt, Tp, Ta, CBR, MDD, IRI	8	SCI	0.0540	Training	0.794
					Validation	0.840
					Test	0.875
					Total	0.813
8-16-1	La, Lb, Lt, Tp, Ta, CBR, MDD, IRI	16	SCI	0.0140	Training	0.789
					Validation	0.862
					Test	0.874
					Total	0.812
8-17-1	La, Lb, Lt, Tp, Ta, CBR, MDD, IRI	17	SCI	0.0128	Training	0.779
					Validation	0.846
					Test	0.853
					Total	0.798



Network	Input variables	Neurons	Output variables	MSE	Stage	R <sup>2</sup>
8-4-4-1	La, Lb. Lt, Tp, Ta, CBR, MDD, IRI	4	SCI	0.0960	Training	0.789
					Validation	0.840
					Test	0.567
					Total	0.755
8-8-8-1	La, Lb. Lt, Tp, Ta, CBR, MDD, IRI	8	SCI	0.0513	Training	0.817
					Validation	0.706
					Test	0.571
					Total	0.754
8-16-16-1	La, Lb. Lt, Tp, Ta, CBR, MDD, IRI	16	SCI	0.1130	Training	0.773
					Validation	0.868
					Test	0.849
					Total	0.794
8-17-17-1	La, Lb. Lt, Tp, Ta, CBR, MDD, IRI	17	SCI	0.0780	Training	0.815
					Validation	0.747
					Test	0.765
					Total	0.795
8-4-1	La, Lb. Lt, Tp, Ta, CBR, MDD, IRI	4	BCI	0.2790	Training	0.702
					Validation	0.705
					Test	0.775
					Total	0.712
8-8-1	La, Lb. Lt, Tp, Ta, CBR, MDD, IRI	8	BCI	0.1510	Training	0.781
					Validation	0.642
					Test	0.778
					Total	0.746
8-16-1	La, Lb. Lt, Tp, Ta, CBR, MDD, IRI	16	BCI	0.1780	Training	0.802
					Validation	0.652
					Test	0.800
					Total	0.777
8-17-1	La, Lb. Lt, Tp, Ta, CBR, MDD, IRI	17	BCI	0.0208	Training	0.793
					Validation	0.662
					Test	0.681
					Total	0.762
8-4-4-1	La, Lb. Lt, Tp, Ta, CBR, MDD, IRI	4	BCI	0.1480	Training	0.738
					Validation	0.512
					Test	0.668
					Total	0.692
8-8-8-1	La, Lb. Lt, Tp, Ta, CBR, MDD, IRI	8	BCI	0.2260	Training	0.752
					Validation	0.775
					Test	0.727
					Total	0.753

Network	Input variables	Neurons	Output variables	MSE	Stage	R <sup>2</sup>
8-16-16-1	La, Lb, Lt, Tp, Ta, CBR, MDD, IRI	16	BCI	0.0290	Training	0.734
					Validation	0.737
					Test	0.720
					Total	0.730
8-17-17-1	La, Lb, Lt, Tp, Ta, CBR, MDD, IRI	17	BCI	0.2540	Training	0.797
					Validation	0.710
					Test	0.586
					Total	0.751

### 8.3.3. Discussion of results

The feed-forward BP-ANN approach in this study has satisfactorily demonstrated the correlation of input and output variables with varying coefficients of determination. It should be noted that the data set used for modeling purposes has not been taken from any synthetic database, rather it has been obtained experimentally by conducting extensive field testing which might have few manual or instrumental errors associated during testing. Therefore, the coefficient of determination (R<sup>2</sup>) values obtained in 0.7-0.8 range can be considered to be indicative of good correlation between the variables. Although it is concluded that the correlation fits well, the R<sup>2</sup> values may be further improved by modifying the non-linearity aspects such as changing the transfer function or number of hidden layers and may be considered in future scope of the study. The intelligent approach of neural networks has been concluded to be felicitous for the complex problems of pavement response modeling, wherein numerous factors play prominent roles. The development of similar robust models would assist the highway agencies in easing the decision-making exercises of pavement maintenance and rehabilitation treatments in a short span of time.

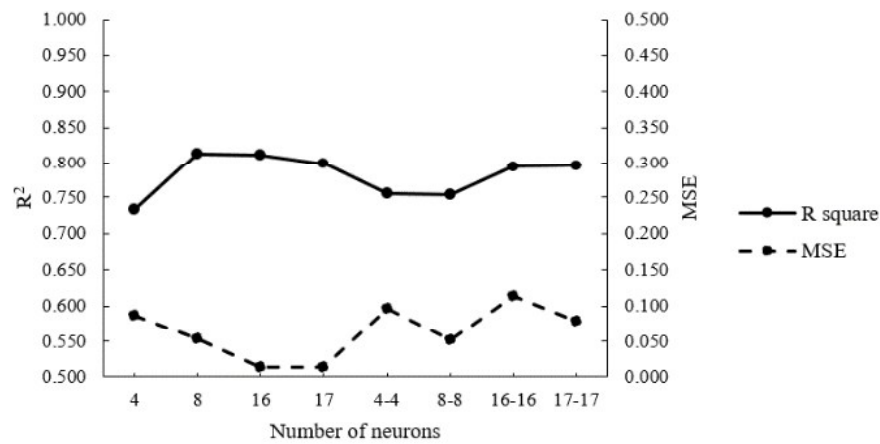
The large dataset and field testing outcomes assure the robustness of these models, and their implementation presents practical field implications. In a general sense, for a model with reasonable accuracy, the R<sup>2</sup> value, which is a measure of the correlation between outputs and targets, is high (close to one), and MSE which is the average squared difference between outputs and targets, is low (close to zero). However, the acceptable values would differ from case to case and depend on the data availability and problem category. The R<sup>2</sup> value of ANN models in this study is obtained to be as good as 0.875, with the average value for all the three samples (training,

validation, and test) being 0.784, 0.810, and 0.768 for SCI; and 0.762, 0.674, and 0.717 for BCI (refer Table 8.3). The satisfactory  $R^2$  value in all the sixteen models proves that the correlation developed in this work is significant, which can be further attested by observing the low values of MSE, presented in Table 8.3. The error distribution plots help to visualize the possible trends and also confirm the results, with an average value close to zero. Another notable finding which compliments the outcomes from literature is that as compared to other pavement layers, properties of asphalt layer have a more profound influence on the condition of pavement (Schwartz et al., 2011). The finding is clearly evident from  $R^2$  values of SCI, which are higher than the  $R^2$  values of BCI. It is worth to note that for the accuracy and acceptability of the model, low values of MSE is not imperative since it is affected by the type of data, degrees of freedom, residual space, and regression. Meticulous investigation of regression, MSE, and error plots should be made before drawing any conclusion regarding the choice of the best network. Theoretically, as number of neurons increases, the ANN model achieves better precision and prediction proficiency, but on the contrary increases complexity and computation time. Nevertheless, with a view to select the best and optimum network architecture from the sixteen structures containing a different number of computational neurons, apart from  $R^2$  and MSE values, the simplicity and computational ease are also taken into consideration.

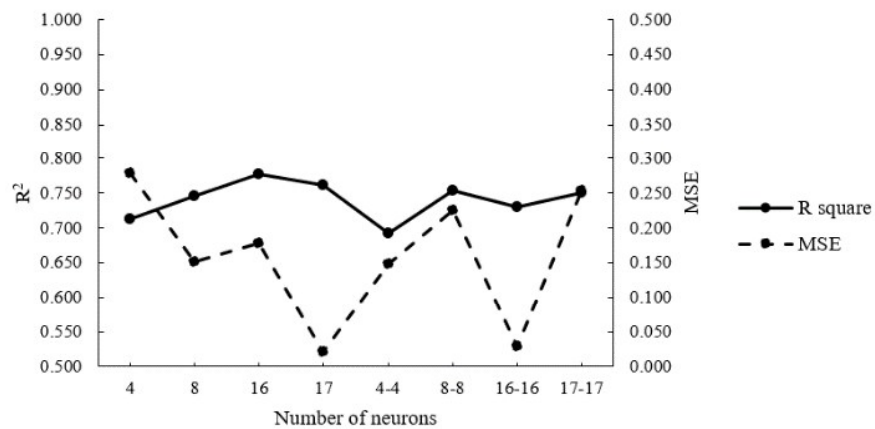
#### **8.3.3.1. Selection of the best network**

In accordance with the selection of the best network architecture, as seen from Table 8.3 and Figure 8.8 the  $R^2$  values obtained for the network structure 8-8-1 and 8-16-1, i.e., for neurons equal to the number of input variables and twice of the number of input variables, are superior as compared to the  $R^2$  values obtained for all other network architectures. On further increasing the number of neurons or number of hidden layers, there is no significant improvement in the performance of the models. For one-layer models with SCI as an output parameter, increasing the number of neurons from 4 to 8, increases  $R^2$  value by 10.76%, whereas on further increment of neurons there is no significant change in  $R^2$  value, and it eventually decreases. With BCI as an output parameter in one-layer models,  $R^2$  value increases by about 4% on increasing the neurons from 4 to 8, and 8 to 16 but decreases by additional neurons. The general trend of MSE values in both the cases is such that it is maximum for 4-neuron models and reduces (approximately by 37% for SCI and 45% for

BCI) with the increase of neurons number to eight. Additionally, it is evident from the  $R^2$  values of one-layer models and two-layer models that the overall performance of the two-layer models is less than the one-layer models. One of the important observation is that even for two-layer models, better performance (in terms of  $R^2$  and MSE values) is obtained for the 8-8-8-1, and 8-16-16-1 structures, i.e., for neurons equal to the number of input variables and twice of the number of input variables but the two layers make the system much more intricate. However, since the results from both the structures are comparable and considering the need to maintain the simplicity of the models by keeping fewer neurons and hidden layers, the network configuration 8-8-1 can be selected as the best structure.



(a) SCI



(b) BCI

**Figure 8.8. Variation in regression and mean square error results for different ANN architectures**

## 8.4. Comparison with multiple linear regression approach

In order to further validate the superiority of ANN for such complex non-linear problems, the ANN results have been compared with multiple linear regression approach, with the same number of input records. Table 8.4 compares the results of multiple linear regression models for SCI and BCI, respectively, with that of the ANN model with 8-8-1 architecture. The  $R^2$  from these models for the same number of records and input variables are 41.60% and 44.10% lower for SCI and BCI, respectively than those obtained from ANN. However, the p-values are almost equal to zero and less than the significance level of 0.05, therefore, a significant linear regression relationship exists between the variables. This provides the evidence to the higher applicability of ANN models for dealing with such non-linear behaviors.

**Table 8.4. Comparison of results from artificial neural networks and multiple linear regression approaches**

	Model type			
	Artificial neural network (8-8-1 structure)		Multiple linear regression	
<b>Input variables</b>	La, Lb, Lt, Ts, Ta, CBR, MDD, IRI		La, Lb, Lt, Ts, Ta, CBR, MDD, IRI	
<b>Output variable</b>	SCI	BCI	SCI	BCI
<b>R<sup>2</sup></b>	0.813	0.746	0.475	0.417
<b>MSE</b>	0.054	0.151	0.032	0.055

The highway agencies may work on a similar fashion by training their own ANN structures using the readily available or measurable data to obtain an accurate prediction of structural adequacy without entirely depending on the deflection tests. However, the results are highly dependent on the number, quality, and characteristics of the input variables. Therefore, the selection of these parameters should be made scrupulously by understanding their connections/relationships.

## 8.5. Concluding remarks

The preliminary approach presented in the study provides reliable correlations among the attributes and facilitate quick estimation of pavement's structural health, by reducing the frequency of

measuring pavement deflections. The ease of approach for data analysis minimizes the need to go through the cumbersome process of back-calculation. The predicted values of deflection basin parameters can be used suitably to draw productive and reliable conclusions regarding the possible structural condition of the pavement layers. This would foster the increased application of structural condition data in pavement maintenance and rehabilitation necessities. Furthermore, decisions about the necessity and suitability of maintenance or rehabilitation selections can be easily made. However, it does not intend to avoid conducting the deflection testing since the direct assessment of structural capacity would indeed increase the model accuracy. Accordingly, future studies can seek to incorporate other significant input parameters such as traffic-related (like annual average daily traffic, equivalent single axle load, etc.), additional climatic factors (like annual average daily temperature), rainfall data, and other functional performance indicators such as pavement condition index, and present serviceability index. The study can form a basis for future studies by incorporation of additional parameters listed above, particularly at network levels where deflection data acquisition and processing frequently is a challenge but the approach and methodology adopted could be similar. It is worth mentioning here that the trained ANN models should be adopted for similar cases only, otherwise the accuracy and quality of prediction could be affected significantly.



This document was created with the Win2PDF "print to PDF" printer available at <http://www.win2pdf.com>

This version of Win2PDF 10 is for evaluation and non-commercial use only.

This page will not be added after purchasing Win2PDF.

<http://www.win2pdf.com/purchase/>